BIOCHEMISTRY
including biophysical chemistry & molecular biology

Article

pubs.acs.org/biochemistry

Nematode Sgt1-Homologue D1054.3 Binds Open and Closed Conformations of Hsp90 via Distinct Binding Sites

Julia M. Eckl, Adrian Drazic, Daniel A. Rutz, and Klaus Richter*

Department of Chemistry, Technische Universität München, 85748 Garching, Germany

Supporting Information

ABSTRACT: Heat shock protein 90 (Hsp90) is a highly conserved ATP-driven machine involved in client protein maturation, folding, and activation. The chaperone is supported by a set of cochaperones that confer client specificities. One of those proteins is the suppressor of G2 allele of *skp1* (Sgt1), which participates together with Hsp90 in the immune responses of plants. Sgt1 consists of three domains: a TPR-, CS-, and SGS-domain, conserved in plants, yeast, and humans. The TPR-domain though is lacking in nematodes and insects. We observe that the *Caenorhabditis elegans* Sgt1 homologue D1054.3 binds to Hsp90 in the absence of nucleotides but much stronger in the presence of ATP and ATPγS. The latter binding mode is similar to p23, another CS-domain containing Hsp90 cofactor, even though binding is not observable for p23 in the absence of nucleotides. We use point mutations in Hsp90, which accumulate different conformations in the ATPase cycle, to differentiate between binding to open and closed Hsp90 conformations. These data support a strong contribution of the Hsp90 conformation to Sgt1 binding and highlight the ability of this cofactor to interact with all known Hsp90 conformations albeit with different affinities.

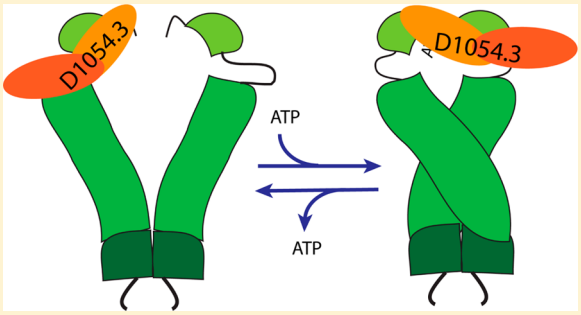

The molecular chaperone heat shock protein 90 (Hsp90) regulates the folding, assembly, maturation, and activation of several hundred client proteins in an ATP-dependent manner.[1,2] Protein kinases, transcription factors, steroid hormone receptors (SHR), and E3-ligases belong to the huge set of Hsp90 clients.[3,4] Hsp90 itself is a homodimer consisting of an N-terminal ATP binding site (Hsp90N), a middle domain assumed to participate in client interaction (Hsp90M), and a C-terminal dimerization domain (Hsp90C), which additionally binds proteins with a tetratricopeptide repeat (TPR) domain with its C-terminal MEEVD motif.[5−7] Upon ATP binding, the N-terminal domains of Hsp90 associate and form a ringlike state, which performs the hydrolysis reaction.[5,6,8] During this closing reaction, the nucleotide binding domains reorient against the middle domain.[9−11] This ATPase cycle is conserved in all known Hsp90 proteins.[5,6] ATP-induced conformational changes are required for client activation. However, it is unknown to date how the client turnover proceeds in detail.[12−14] It is well described that distinct classes of clients need specific cochaperones. As such, kinases require the Hsp90 cofactor Cdc37 (cell division cycle 37),[15−18] whereas SHR activation is more efficient in the presence of p23.[19,20] Both cochaperones affect the ATPase activity of Hsp90 and additionally contact the respective client proteins. So far, about 20 cofactors for Hsp90 have been described.[7,8]

Suppressor of G2 allele of *skp1* (Sgt1) is an Hsp90 cochaperone that also acts as a client adaptor protein. It has been mainly characterized in plants and yeast and is involved in formation of the kinetochore complex, ubiquitinylation processes, activation of the cyclic AMP pathway, stabilization of the Polo kinase, and regulation of the immune response.[21−26] Sgt1 consists of three domains—a TPR-domain, a CHORD/SGT1-domain (CS), and a SGT1-specific domain (SGS). The protein can homodimerize via its TPR-domain, which is necessary for yeast kinetochore assembly.[21,27,28] Several other proteins also bind to the TPR-domain of Sgt1, such as Skp1, which is part of the SCF (Skp1/Cullin/F-box) E3 ubiquitin ligases.[29] Initially, it was assumed that the TPR-domain mediates the Hsp90 interaction and binding occurs by the recognition of the C-terminal MEEVD motif of Hsp90 similar to other TPR-domain containing cochaperones.[22] More recent studies suggest that the CS-domain interacts with the Hsp90N domain[30,31] similar to the Hsp90-cofactor p23, which utilizes a CS-domain for Hsp90 binding.[6] In the crystal structure of Hsp90N in complex with the CS-domain of Sgt1a, two potential binding interfaces can be observed.[31] Mutation studies suggest an interaction with the N-terminal amino acids of Hsp90. Beyond binding Hsp90, the CS-domain of Sgt1 additionally binds to Rar1. This interaction is required for disease resistance involving the *n*ucleotide-binding site and *l*eucine-rich repeat domain containing *r*eceptors (NLR) as clients.[32−34] The molecular chaperone Hsp70 also interacts with the SGS-domain of Sgt1.[35,36]

Despite its essential nature in yeast,[24,28] we surprisingly had not identified a Sgt1-like TPR-protein in the nematode

Received: January 13, 2014
Revised: March 12, 2014
Published: March 24, 2014

   dx.doi.org/10.1021/bi5000542 | *Biochemistry* 2014, 53, 2505−2514

Caenorhabditis elegans.[7] In contrast, the single Sgt1 homologue in *C. elegans*, D1054.3, lacks the TPR-domain but contains CS- and SGS-domains with high similarity to the human Sgt1 protein. In this study, we analyze the interaction of D1054.3 with Hsp90 to characterize the remaining interaction sites with Hsp90 and develop a concept for the interaction mechanism in the absence of the TPR-domain.

MATERIALS AND METHODS

Gene Bank Analysis of Sgt1-Homologues. BLAST searches employing http://blast.ncbi.nlm.nih.gov/Blast.cgi were used to obtain sequence information on metazoan Sgt1-homologues. To this end, we used known Sgt1-homologues as input sequences for the queries. Searching all eukaryotic sequences (Eukaryota, taxid: 2759), we obtained many Sgt1-homologues, all with an alignment score of at least 80. Classes without identified homologue due to insufficient genome sequencing were omitted in our phylogenetic tree. Beyond the CS- and SGS-domains, we inspected all found homologues whether they contained other domains which bear similarity to a TPR-domain. Searching Metazoa/Animalia (taxid: 33208), we still obtained both forms of Sgt1-homologues. In one phylum (Arthropoda, taxid: 6656),1 we obtained a mixture of TPR-domain containing Sgt1-homologues and TPR-domain free homologues. In this case, we queried Sgt1-homologues within the respective classes. This way we obtained a phylogenetic tree of metazoa, containing information on the presence of the Sgt1 TPR-domain in the different branches.

Cloning, Protein Expression and Purification. The *C. elegans* proteins D1054.3, ZC395.10 (Cep23, homologue of p23/Sba1), STI-1, DAF-21/C47E8.5 (homologue of Hsp90), its mutants F10A-Hsp90, L17A-Hsp90, Y26A-Hsp90, Q111A-Hsp90, F340E-Hsp90, and R372A-Hsp90, all Hsp90 fragments (Hsp90N, Hsp90M, Hsp90C, Hsp90NM, and Hsp90MC), and C01G10.8 (CeAha1, homologue of Aha1) were purified according to established protocols with an N-terminal His_6-tag (Supplemental Figure 1, Supporting Information).[17,37,38] cDNAs for these proteins were obtained from Open Biosystems (Thermo Fisher, USA) and sequenced to confirm the amino acid sequence provided by www.wormbase.org. The coding sequences were cloned into a pet28b bacterial expression vector and transformed in BL21-Cod+ (DE3) RIL cells. These were grown at 37 °C to an A_{600} of 0.8. Protein expression was induced by adding 1 mM IPTG to the culture. After induction, cells were harvested and lysed in a TS 0.75 cell disruption instrument (Constant Systems, Ltd., Northants, UK), and the proteins were purified in three steps. First, the His_6-tagged protein was applied to a HisTrap FF 5-mL column (GE Healthcare), and the protein was eluted with 300 mM imidazole. Next, the protein was purified on a ResourceQ (GE Healthcare) ion exchange column, and finally size exclusion chromatography was performed using a Superdex75 HiLoad column (GE Healthcare). The His_6-tag was not removed from the proteins, as extensive studies of yeast and human Hsp90 proteins had shown that this tag does not alter functionality.[5,39] A solution of 40 mM HEPES/KOH pH 7.5, 20 mM KCl, 1 mM DTT was used as storage buffer. The quality of each purified protein was confirmed by SDS-PAGE and MALDI TOF mass spectrometry.

ATPase Activity Assays. ATPase activity assays were performed to determine the ATP turnover of Hsp90 alone and in the presence of cochaperones.[40] Measurements were performed at 25 °C in a buffer containing 40 mM HEPES/KOH pH 7.5, 20 mM KCl, and 5 mM $MgCl_2$ and the ATPase assay components pyruvate kinase, phosphoenolpyruvate, NADH, and lactate dehydrogenase (Roche Applied Science). The NADH absorbance was recorded at 340 nm. For each reaction, 3 μM Hsp90 was used in combination with 6 μM D1054.3 or 6 μM Cep23 and 2 μM CeAha1 or as indicated. To start the reaction, 2 mM ATP was added. Putative background activities were detected by the Hsp90 specific inhibitor radicicol (Sigma-Aldrich). Fits for titrations were performed as described previously.[41] The Hsp90 ATPase activity was calculated using the following equation:

$$\text{activity} = \frac{\frac{\Delta A_{340}}{\Delta t} - \frac{\Delta A_{340}}{\Delta t_{\text{background}}}}{(\varepsilon(\text{NAD}^+) - \varepsilon(\text{NADH}))c[\text{ATPase}]}$$

Fluorescent Labeling of D1054.3 and p23. Fluorescently labeled *D1054.3 was generated by mixing purified D1054.3 with AlexaFluor 488 C5-maleimide (Alexa488) (Invitrogen) followed by incubation at room temperature for 1 h. *Cep23 was labeled similarly with 5(6)-carboxyfluorescein (FAM) (life technologies, Darmstadt, Germany). Labels were added in a 3-fold molar excess to 1 mg of protein in a buffer containing 40 mM HEPES/KOH pH 7.5, 20 mM KCl. The reaction was stopped with either 20 mM DTT (for *D1054.3) or 20 mM Tris/HCl pH 8.0 (for *p23). The free label was separated from the labeled protein on a Superdex 75 HR column (GE Healthcare). The concentration and degree of labeling (DOL) were determined with the following equations using the documented parameters for the two labels ($CF_{280,FAM}$ = 0.30; ε_{FAM} = 68 000 M^{-1} cm^{-1}; $CF_{280,Alexa488}$ = 0.11; $\varepsilon_{Alexa488}$ = 71 000 M^{-1} cm^{-1} according to the manufacturer):

$$A_{\text{Prot}} = A_{280} - A_{\text{max}}\text{CF}$$

$$\text{DOL} = \frac{A_{\text{max}}}{[\text{protein}]\varepsilon_{\text{dye}}}$$

Analytical Ultracentrifugation with Fluorescently Labeled Proteins. Analytical ultracentrifugation (aUC) experiments were performed in a Beckman ProteomeLab XL-A equipped with a fluorescence detection system (Aviv Biomedical, Lakewood, NY) and a Ti-50 rotor (Beckman Coulter, Brea) at 20 °C and 42 000 rpm. Samples contained either 250 nM *p23 or *D1054.3. The complex formation with another protein was detected by adding 3 μM of the unlabeled putative binding partner. Optionally 4 mM nucleotides were added. In competition assays, 10 μM unlabeled D1054.3, p23 or Hsp90 fragments were added to the samples. All measurements were carried out in a buffer containing 40 mM HEPES/KOH pH 7.5, 20 mM KCl, 1 mM DTT, and 5 mM $MgCl_2$ unless indicated otherwise. Evaluations were performed using dc/dt analysis as described.[42] To obtain the $s_{20,w}$ values, the plots were fitted with a bi-Gaussian function. Alternatively the C(s) analysis module of UltraScan[43,44] was used to obtain percentage values for the free protein and complexed species in the sample.

Cross-Linking Experiments with Fluorescently Labeled Proteins. Cross-linking experiments were performed using the cross-linker glutardialdehyde. Either labeled *D1054.3 or *p23 (500 nM) were preincubated alone or in combination with 3 μM Hsp90 in 40 mM HEPES/KOH pH 7.5, 20 mM KCl, 1 mM DTT, and 5 mM $MgCl_2$ at 25 °C. The nucleotide ATPγS was used at a concentration of 2 mM. The cross-linking reaction was started by adding 1 μL of 2.5%

glutardialdehyde to the 12 μL sample followed by an incubation time of 10 min. Cross-linking was stopped by addition of 1 M Tris pH 8.5 buffer. Samples were analyzed using precast SDS-PAGE gradient gels (Serva), and the fluorescent bands were visualized using a Typhoon phosphor- and fluorescence imager (GE Healthcare) with the settings appropriate for AlexaFluor 488.

Anisotropy Assay with *p23. Fluorescence anisotropy (FA) assays were performed using a Fluoromax F3 fluorescence spectrophotometer (Horiba Scientific). The assays were carried out in a buffer containing 40 mM HEPES/KOH pH 7.5, 20 mM KCl, 1 mM DTT, and 5 mM $MgCl_2$ at 25 °C. *p23 (250 nM) was preincubated with 2 μM Hsp90 or one of its mutants. The fluorescence signal was excited at 494 nm and detected at 518 nm with a time increment of 0.3 s. Polarization filters were set to the magic angle. After the baseline was observed for a few minutes, the kinetics was started by adding 2 mM ATPγS. *p23 binding was observed by an increase in the anisotropy. After the signal reached plateau values, 6 μM unlabeled p23 or D1054.3 was added to disrupt the *p23−Hsp90 complex again. Data analysis was carried out using single-exponential functions in the Origin 8 software.

Thermo Stability Assay (TSA). The assay was measured in a 96-well plate. Each well contained 0.2 mg/mL of protein of interest and 2 μL of a 1:1000 (v/v) dilution of the environmental sensitive fluorescent dye SYPRO orange in a total volume of 20 μL. Measurements were performed in 40 mM HEPES/KOH pH 7.5, 20 mM KCl, and 1 mM DTT. The dye was excited at a wavelength of 470 nm, and fluorescent emission was detected at 570 nm. The temperature was increased in 131 cycles from 25 °C with 0.5 °C per cycle.

RESULTS

Loss of the Sgt1 TPR-Domain Occurred in Several Events in Metazoa. Sgt1 is known to play a major role in cell cycle processes and the innate immune response of plants and animals.[21−23] The protein itself is well conserved. It usually consists of three domains: a TPR-domain, a CS-domain, and the Sgt1-specific SGS-domain. We were surprised to see that the nematode homologue D1054.3 lacks the N-terminal TPR-domain, while the CS- and SGS-domains are conserved. D1054.3 shows a query cover of 97% and a sequence identity of 37% to the human protein, within the CS- and SGS-domains. We searched within the metazoan kingdom for Sgt1-homologues with similar structures and visualized the results in a phylogenetic tree (Figure 1). The tree shows only classes that contain homologues with an alignment score of at least 80. The phyla and classes, which are lacking the TPR-domain but still contain the CS- and SGS-domain, are marked in red, while those containing the TPR-domain are marked in green. Interestingly, in some branches, for example, in arthropoda, the TPR-domain of Sgt1 is missing in one group (insects) but is present in the other (crustacea) even though these organisms are closely related. So, while the TPR-domain is present in *Saccharomyces cerevisiae*, *Schizosaccharomyces pombe*, *Arabidopsis thaliana*, *Homo sapiens*, and *Mus musculus*, it is absent in *C. elegans*, *Drosophila melanogaster*, and flatworms. As both forms appear in the arthropod phylum, it is likely that this TPR-domain was lost on several occasions during evolution, implying that the TPR-domain may be dispensable for the functionality of Sgt1 in certain organisms. This is supported by observations that the TPR-domain is not required for plant immunity and auxin signaling.[21,27,29,45] Therefore, it is likely

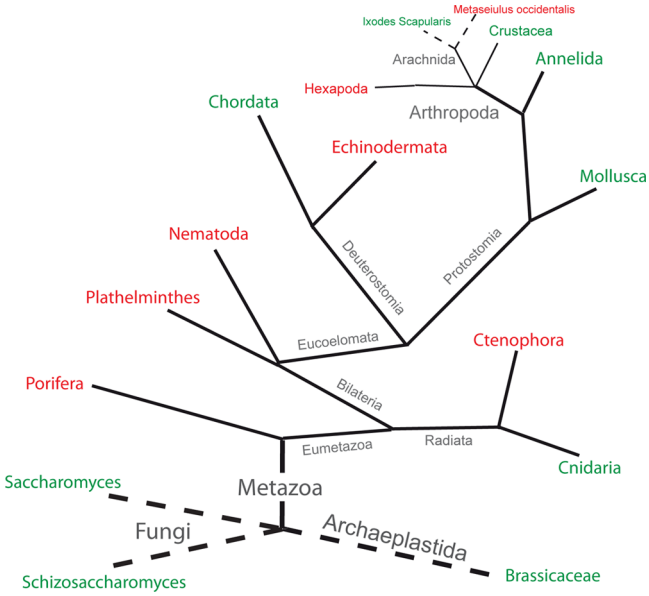

Figure 1. Phylogenetic analysis of Sgt1-domains. Sgt1-homologues of metazoa were analyzed in BLAST searches regarding the presence of the TPR-domain. The presence of a TPR-domain is marked in green, whereas the absence is highlighted in red.

that the CS-domain and the SGS-domain, present in the nematode D1054.3, perform the most relevant functions of Sgt1.

D1054.3 Interacts with Hsp90 in the Presence and Absence of Nucleotides. Given the two potential Hsp90-interacting domains in traditional Sgt1-homologues, we wondered whether the loss of the TPR-domain affects the interaction with Hsp90. To study this, we fluorescently labeled D1054.3 (*D1054.3) and performed cross-linking experiments with Hsp90. For comparison, we did the same experiments with the CS-domain containing cofactor Cep23 (labeled *p23), which is binding Hsp90 via this CS-domain. We cross-linked both labeled proteins with Hsp90 alone and in the presence of ATPγS (Figure 2A). *p23 generated more cross-linking product with Hsp90 in the presence of ATPγS, implying that the interaction of nematode p23 is better in the closed state of Hsp90. This behavior is very similar to p23-like proteins from other organisms.[46−49] *D1054.3 likewise cross-links strongly to Hsp90 in the presence of ATPγS but also forms a cross-linking product if nucleotides are omitted implying that both proteins bind in a nucleotide-dependent interaction.

To confirm this mode of interaction, an aUC experiment was performed with *D1054.3. Hsp90 was added alone or in combination with different nucleotides (Figure 2B). These experiments confirmed that *D1054.3 forms a complex with Hsp90 in the absence of nucleotides or with ADP but much stronger in the presence of ATPγS, while the presence of ATP resulted in intermediate complex formation (Figure 2B). Then, we tested *p23, which in yeast and human species only can be incorporated into Hsp90 complexes in the presence of the nonhydrolyzable nucleotide analogues AMP-PNP or ATPγS. *p23 binds strongly, if nematode Hsp90 is closed by addition of ATPγS. Despite this, it also binds Hsp90 in the presence of ATP (Figure 2C). As expected, *p23 binding in the absence of nucleotides or in the presence of ADP was not detectable (Figure 2C). The observed p23−Hsp90 interaction in the presence of ATP differs from results with yeast Hsp90, where

dx.doi.org/10.1021/bi5000542 | *Biochemistry* 2014, 53, 2505−2514

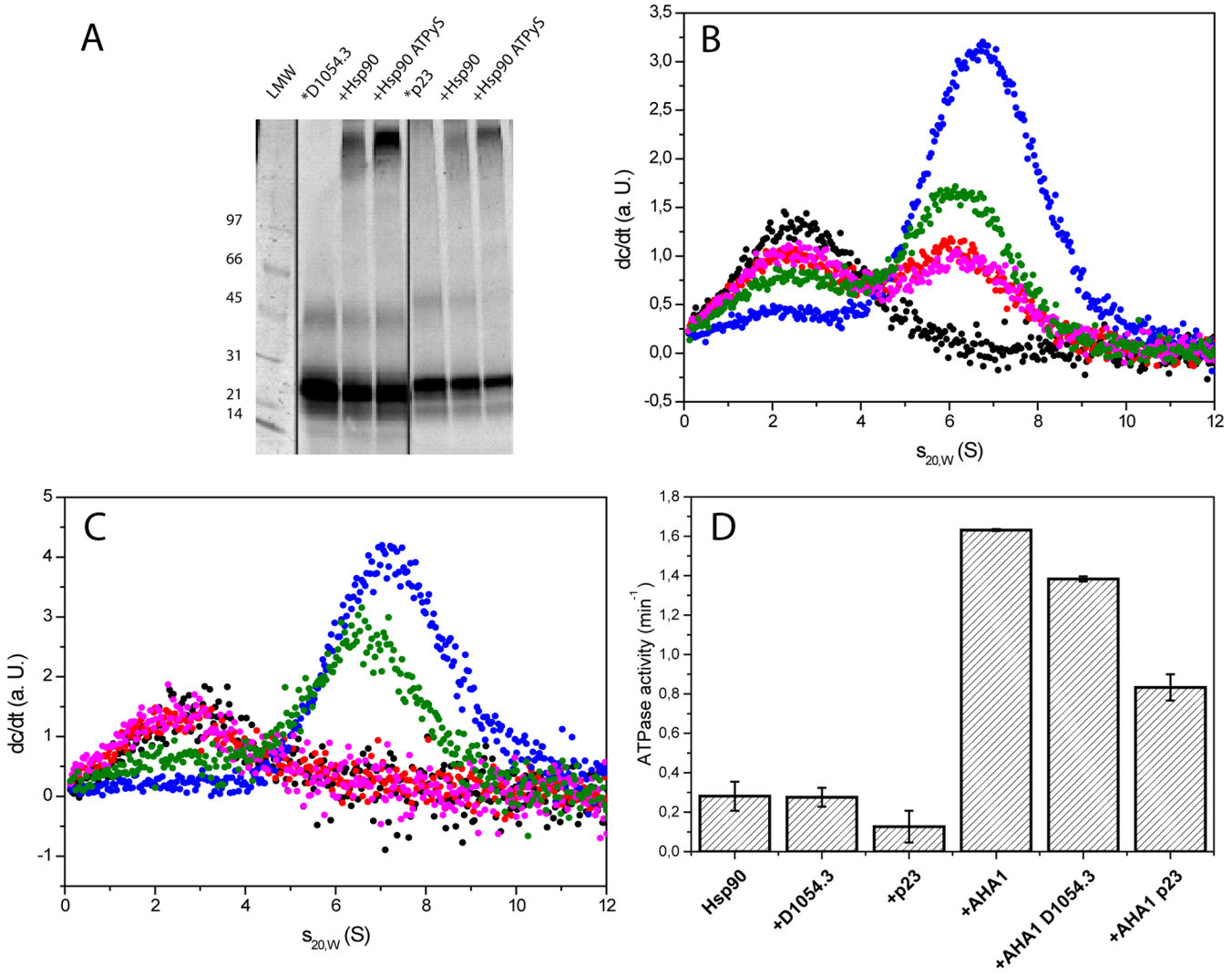

Figure 2. Nucleotide-dependent binding of D1054.3 to Hsp90. (A) Chemical cross-linking of 500 nM labeled *D1054.3 or *p23 and 3 μM Hsp90 in the presence or absence of 2 mM ATPγS was performed with glutardialdehyde. (B) aUC experiment of 250 nM labeled *D1054.3 alone (black), with 3 μM Hsp90 (red), and after the addition of 4 mM nucleotides to the Hsp90–D1054.3 complex (ADP – magenta, ATP – green, and ATPγS – blue. (C) The same aUC experiment was performed for labeled *p23 (black) with the same Hsp90 conditions as for *D1054.3. (D) ATPase activity assay of 3 μM Hsp90 alone and in combination with 6 μM D1054.3 or p23 and 2 μM CeAha1 was measured at 25 °C. All measurements were performed in 40 mM HEPES/KOH pH 7.5, 20 mM KCl, 1 mM DTT, and 5 mM $MgCl_2$ (standard assay buffer).

the addition of ATP does not result in sufficient accumulation of the closed Hsp90-conformation, a feature apparently different for the nematode Hsp90 protein.[46−49]

Observing that both proteins are able to interact with Hsp90, we were interested in their regulatory role during the Hsp90 ATPase cycle. The cochaperone p23 is known to weakly inhibit the ATPase activity of yeast Hsp90, but given the apparent differences between nematode and yeast Hsp90, the affinities and mechanisms could be altered. We find that also *C. elegans* p23 decreases the ATP turnover of CeHsp90 (Figure 2D). Upon addition of the activator CeAha1, an increase in activity is detected, while a supplementation with p23 leads again to a significant decrease in activity. Thus, Cep23 acts as an efficient inhibitor of the stimulated and unstimulated ATPase of Hsp90 (Supplemental Figure 3, Supporting Information). To test whether D1054.3 could influence this activity, we performed ATPase assays using the same experimental setup (Figure 2D). This time, no change in Hsp90 ATPase activity was observed and also in the presence of CeAha1, D1054.3 was very inefficient compared to p23 in decreasing the ATP turnover (Supplemental Figure 3).

D1054.3 and p23 Have an Overlapping Binding Site for Hsp90 in Its Closed Conformation. To understand the differences in ATPase inhibition and nucleotide dependency, we directly compared the binding properties of D1054.3 and Cep23. This is interesting as crystallographic studies had proposed different interaction sites for the two CS-domain containing proteins,[31] and other studies had suggested a stronger binding of Sgt1 to the nucleotide-free state of Hsp90.[31]

To test whether D1054.3 and p23 have overlapping binding sites, we used our aUC set up with either labeled *p23 or *D1054.3 and assembled a complex with Hsp90 and ATPγS (Figure 3A,B). Then we tried to compete against complex formation with unlabeled D1054.3 or p23, respectively. *p23 can be fully displaced by unlabeled p23 showing the specificity of the observed interaction (Figure 3A). Instead, *p23 can barely be displaced by unlabeled D1054.3 suggesting a higher

dx.doi.org/10.1021/bi5000542 | *Biochemistry* 2014, 53, 2505−2514

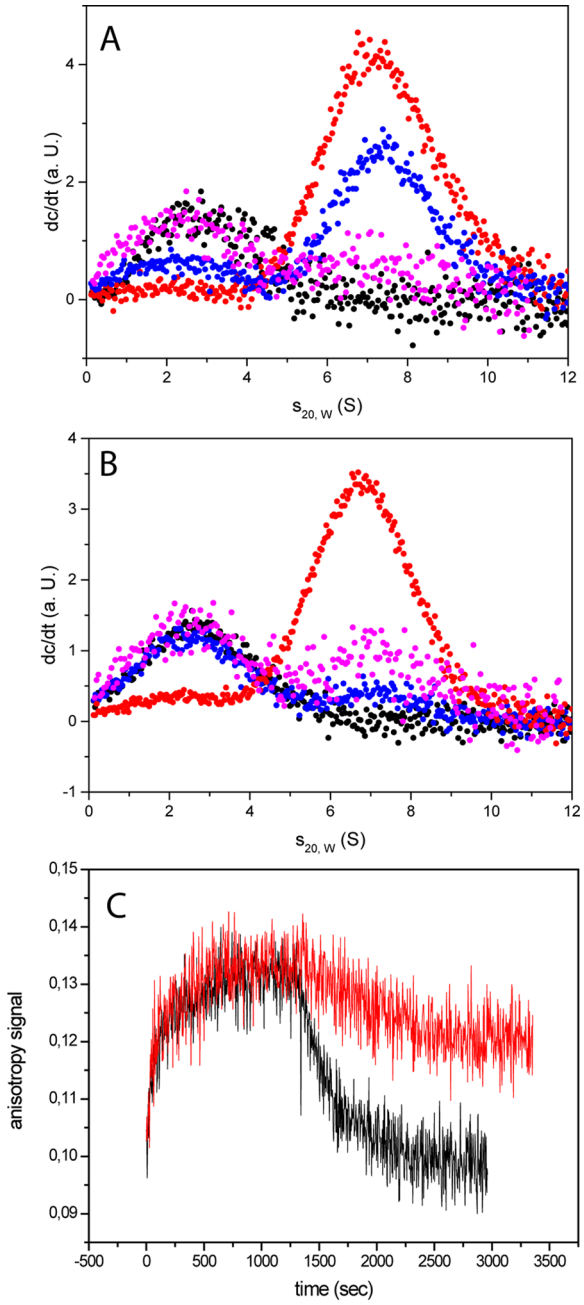

Figure 3. D1054.3 and p23 have an overlapping binding site. (A) aUC experiment with 250 nM labeled *p23 alone (black) or in the presence of 3 μM Hsp90 + 4 mM ATPγS (red). The resulting complex was challenged with 10 μM D1054.3 (blue) or 10 μM p23 (magenta). (B) The same experiment as in A was performed for 250 nM labeled *D1054.3 (black). The complex with 3 μM Hsp90 + 4 mM ATPγS (red) was challenged with 10 μM p23 (blue) or 10 μM D1054.3 (magenta). (C) The kinetic of the *p23 (250 nM)−Hsp90 (2 μM) interaction was observed in an anisotropy assay at 25 °C. The measurement was started by adding 2 mM ATPγS and detected until a plateau was reached. Then 6 μM unlabeled p23 (black) or D1054.3 (red) was added. All assays were performed in 40 mM HEPES/KOH pH 7.5, 20 mM KCl, 1 mM DTT, and 5 mM $MgCl_2$.

affinity of the p23−Hsp90 interaction (Figure 3A). On the other hand, unlabeled p23 was able to displace *D1054.3 from the complex with Hsp90−ATPγS in a similar manner as unlabeled D1054.3 itself does (Figure 3B). Thus, both proteins have overlapping binding sites in the closed conformation. We further tested the displacement of D1054.3 from Hsp90 in the absence of nucleotides. And indeed under these conditions, Cep23 does not have an effect, highlighting that binding to this Hsp90 conformation is unique to D1054.3 (data not shown).

To get more information on the binding events, we also performed anisotropy assays. We preincubated *p23 together with Hsp90 and started the kinetics by adding ATPγS (Figure 3C). Inducing the closed conformation, we determined the binding kinetic for the complex formation with a rate of 0.23 ± 0.01 min^{-1}, which in the yeast system reflects the closing rate of Hsp90 and the generation of the *p23 binding interface.[50] ATP addition also leads to an observable binding kinetic with a rate of 1.16 ± 0.11 min^{-1}, but lower amplitude compared to ATPγS. We then tried to disturb the Hsp90−ATPγS−*p23 complex by adding an excess amount of unlabeled Cep23. This reduces the signal back to baseline levels with a rate of 0.25 ± 0.02 min^{-1}, implying efficient displacement of the labeled *p23. We also performed this competition experiment with unlabeled D1054.3, resulting in a much weaker decrease of the signal. Apparently, D1054.3 is barely able to compete with *p23 for Hsp90−ATPγS also in this assay. These data confirm that the affinity of the overlapping binding site on closed Hsp90 is much higher for Cep23, while the binding site on nucleotide-free Hsp90 is only detectable for D1054.3.

The N-Domain Represents a Interaction Site for D1054.3 on Open Hsp90. We wanted to know how the unique binding site of D1054.3 with Hsp90 is built and whether it requires a closing of Hsp90s N-terminal domains. To this end, we compared the binding of *D1054.3 to full-length Hsp90 and to a fragment, which lacks the C-terminal dimerization site (Hsp90NM) in the aUC (Figure 4). We titrated these proteins and obtained binding events detectable through a sharp increase of the $s_{20,w}$ after addition of Hsp90 (Figure 4A) or Hsp90NM (Figure 4B). These data highlight an interaction with the N-terminal and middle domain of Hsp90. The $s_{20,w}$ value of 3.9, as obtained for the complex with Hsp90−NM, strongly argues against any D1054.3 induced dimerization of the N-terminal domains but hints at a monomeric assembly. Addition of ATPγS, which would further support N-terminal dimerization reactions, did not lead to higher sedimentation values in the case of Hsp90−NM (data not shown). The dimeric C-terminal part of Hsp90 (Hsp90C) and Hsp90MC did not show complex formation in the aUC (Supplemental Figure 3). This result suggests that the N-terminal domain and possibly the linker region is a relevant binding site for D1054.3.

Single-Amino Acid Mutants of Hsp90 Highlight the Conformational Control of the D1054.3 Interaction. Having seen the differences in nucleotide dependency, we aimed at utilizing Hsp90 point mutants, which favor different conformational states to reveal the influence of Hsp90 conformations on the binding affinities. To this end, we generated Hsp90 mutants in domain interfaces. Four of the mutants were located in the N-terminal domain of Hsp90 in parts involved in ATP hydrolysis (F10A-Hsp90, L17A-Hsp90, Y26A-Hsp90, Q111A-Hsp90). Two mutants were placed in the middle domain (F340E-Hsp90, R372A-Hsp90), where they form part of the N-M domain interface during ATP hydrolysis.[51] All mutants were stable proteins in thermal transitions (Table 1). The mutants F10A-Hsp90, Y26A-Hsp90, Q111A-Hsp90, F340E-Hsp90, and R372A-Hsp90 showed strongly reduced ATPase activities, implying that their ATPase cycles are blocked at a certain step. Of these mutants, F10A-Hsp90 can be strongly stimulated by CeAha1, suggesting that

dx.doi.org/10.1021/bi5000542 | *Biochemistry* 2014, 53, 2505−2514

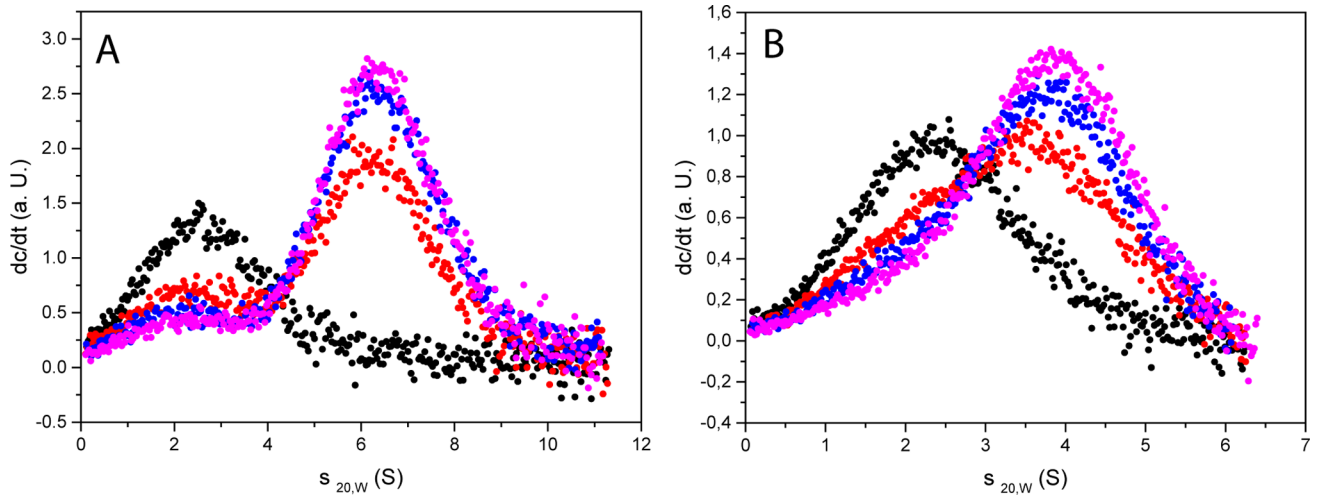

Figure 4. The binding site of D1054.3 is in the N-terminal and middle domain of Hsp90. aUC experiment was performed with 1 μM labeled *D1054.3 (black) in complex with A. increasing Hsp90 (A) and Hsp90NM (B) concentrations (5 μM – red, 10 μM – blue, and 15 μM – magenta).

Table 1. ATPase Activity and Cofactor Interactions of Hsp90 and Its Mutants[a]

	T_m (°C)	ATPase (min^{-1})	ATPase + Aha1 (min^{-1})	p23 + ATP K_D (μM)	p23 + ATPγS K_D (μM)	anisotropy p23*/ATPγS amplitude A	conclusion	D1054.3 K_D (μM)	D1054.3 + ATP K_D (μM)	D1054.3 + ATPγS K_D (μM)
Wt Hsp90	43	0.24 ± 0.02	1.95 ± 0.08	2.5 ± 0.7	0.7 ± 0.4	0.055 ± 0.001		18 ± 4.3	5.0 ± 2.8	2.1 ± 0.8
F10A	45	0.02 ± 0.04	0.97 ± 0.38	7.2 ± 2.6	0.8 ± 0.3	0.028 ± 0.001	activity limited by closing	≫100	60 ± 18	13 ± 4.2
L17A	48	0.19 ± 0.03	3.26 ± 0.25	3.6 ± 0.6	1.0 ± 0.8	0.046 ± 0.001	like Wt	89 ± 19	5.8 ± 2.0	3.6 ± 1.5
Y26A	49	0.02 ± 0.05	0.09 ± 0.10	0.9 ± 0.1	0.5 ± 0.5	0.043 ± 0.001	activity limited by hydrolysis	38 ± 6.9	3.3 ± 1.0	3.3 ± 2.4
Q111A	41	0.02 ± 0.04	0.13 ± 0.19	1.5 ± 0.9	5.0 ± 1.2	0.015 ± 0.002	ATPγS inefficient	38 ± 16	8.1 ± 3.4	14 ± 3.2
F340E	44	0.02 ± 0.02	0.03 ± 0.03	≫100	≫100		no closing	11 ± 4.1	9,4 ± 4.8	5.2 ± 2.7
R372A	42	0.02 ± 0.02	0.17 ± 0.26	2.8 ± 0.6	5.0 ± 0.9	0.026 ± 0.001	ATPγS inefficient	22 ± 6.2	7.1 ± 2.9	8.3 ± 2.5

[a]All Hsp90 mutants show the same thermal stability as wild type Hsp90 in the TSA assay. For each of them, the ATPase activity alone and in the presence of Aha1 is listed. The interaction of 250 nM labeled *p23 and *D1054.3 with 3 μM Hsp90 and its mutants in the presence and absence of 4 mM nucleotides (ATP, ATPγS) was determined in aUC experiments. Binding kinetics of 250 nM *p23 with 2 μM Hsp90 and all mutants was recorded in anisotropy assays. All values were obtained using the equations listed in Materials and Methods.

the initial conformational changes are decelerated compared to the wild type protein. The other mutants barely react to the presence of CeAha1 (Table 1, Figure 5A). To determine, whether these mutants are able to close the N-terminal domains at all, we performed binding assays with Cep23. Using ATP as nucleotide, we observed similar or better binding than wild type for Q111A-Hsp90, R372A-Hsp90, and Y26A-Hsp90 and the absence of binding for F340E-Hsp90 (Table 1). This suggests that Q111A-Hsp90, Y26A-Hsp90, and R372A-Hsp90 are decelerated at the moment of ATP hydrolysis in the closed state and thus accumulate a conformation, which is favorable for p23 binding. In ATPγS complexes, the binding is weakened for Q111A-Hsp90 and R372A-Hsp90 as these mutants seem to be unable to close fully with the nonhydrolyzable nucleotide. The inability of F340E-Hsp90 to bind Cep23 in the presence of ATPγS suggests that in accordance with previous results[38] this mutant is unable to form the closed state (Table 1).

We aimed at confirming the Cep23-binding using the anisotropy assay. This way we determined the closing kinetics of these mutants after addition of ATPγS. Indeed, we observed lower amplitudes for the mutants R372A-Hsp90 and Q111A-Hsp90 and the absence of binding for F340E-Hsp90 (Table 1, Figure 5B) reflecting weaker binding to these mutants. Also binding to F10A-Hsp90 was compromised reflecting potential difficulties during the closing reaction (summarized in Table 1, Figure 5B).

We used this set of mutants to study the conformational states of the D1054.3–Hsp90 interaction (Table 1). Here in particular the mutants Q111A-Hsp90 and R372A-Hsp90 may be useful as they show inverted responses to the nucleotides ATP and ATPγS. Similar to p23, D1054.3 shows almost wild type-like binding in the presence of ATP, while a weaker affinity compared to wild type Hsp90 is observable in the presence of ATPγS. This correlation suggests that the nucleotide-induced closing reaction in both cases is relevant to obtain the high affinity conformation. F340E-Hsp90 instead shows similar binding affinities independent of nucleotide addition, which is in agreement with the notion that no closing reaction can be performed by this mutant. Thus, these mutants highlight that the binding of nucleotide is not the cause of the higher affinity but the conformational changes that are induced by it.

No correlation can be observed with D1054.3 binding to nucleotide-free Hsp90 instead. Here, F10A-Hsp90 and L17A-Hsp90 show weaker binding in the absence of nucleotides. The phenylalanine at position 10 had been proposed earlier to be

dx.doi.org/10.1021/bi5000542 | Biochemistry 2014, 53, 2505–2514

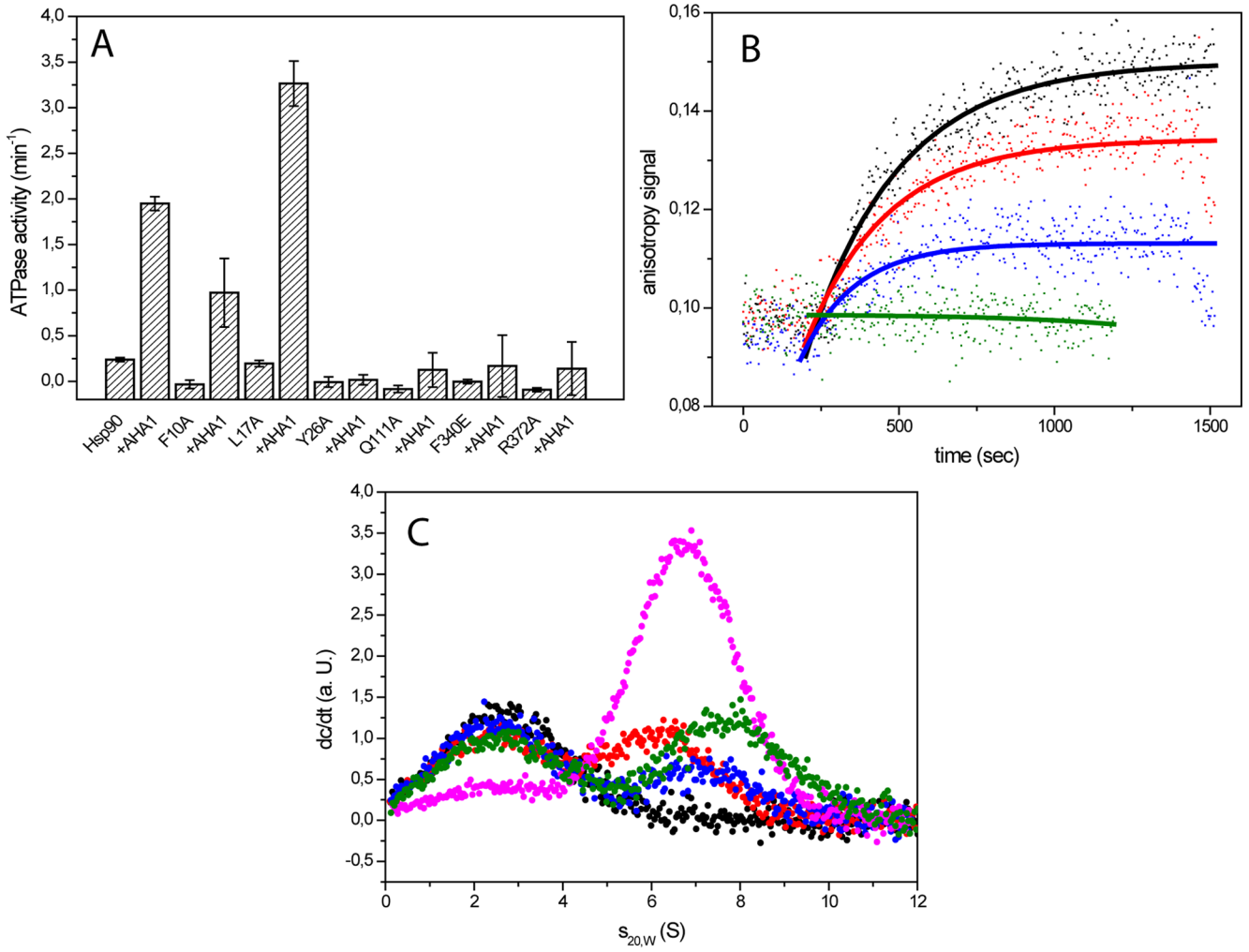

Figure 5. Influence of different Hsp90 mutants on p23 and D1054.3 interaction. (A) The ATPase activity of 3 μM of the analyzed Hsp90 mutants is shown alone and in the presence of the activator CeAha1. (B) An anisotropy binding assay was performed with 250 nM *p23 and 2 μM Hsp90 (black) or some of its mutants (Y26A-Hsp90 – red, F340E-Hsp90 – green, R372A-Hsp90 – blue). The binding kinetics was started by adding 2 mM ATPγS. All assays were performed in standard assay buffer at 25 °C. Panel C shows the simultaneously binding of STI-1 and D1054.3 on Hsp90 in the aUC. The complex between 250 nM *D1054.3 (black) and 3 μM Hsp90 in the open form is depicted in red and in the closed form with 4 mM ATPγS in magenta. Addition of 6 μM STI-1 leads to changes in the dc/dt profiles in the open conformation of Hsp90 (blue) and in the closed form (green).

part of the binding site for Sgt1.[31] To some extent, this appears to be also true for L17 which binds with reduced affinity in the absence of nucleotides but shows wild type-like affinity in the closed state. In the other mutants, the affinity of nucleotide-free Hsp90 to D1054.3 is almost wild type-like. Thus mutations that are functional in their ATPase cycle and conformational rearrangements can be compromised in D1054.3 binding in the open state. On the other hand, Hsp90 mutants compromised for D1054.3 interaction in the closed state are able to interact normally in the open state. This strongly suggests two entirely different interaction modes.

To confirm the conformational control, we utilized the cofactor STI-1, which is known to enforce the open state of the full-length protein (Figure 5C). Indeed, this cofactor weakens the interaction of D1054.3 with closed Hsp90-ATPγS but barely affects the affinity to nucleotide free Hsp90. Instead, it induces a shift to higher $s_{20,w}$ values highlighting its ability to become part of a ternary complex with D1054.3–Hsp90. Thus, these cofactor dependencies highlight the conformational control over the affinity of the nematode Sgt1-homologue to Hsp90.

DISCUSSION

The Sgt1-homologue protein from nematodes, D1054.3, like many Sgt1 proteins from metaozoa, lacks the TPR-domain, which is present in most Sgt1 proteins from yeast to human. The remaining two domains contain the interaction site with Hsp90 and apparently represent the major functional unit of this protein. On the basis of the interaction pattern described herein, we find D1054.3 to interact with the open and the closed state of Hsp90. This is in contrast to the other CS-domain containing protein p23, which exclusively binds the closed state.[46−49] Thus, our data on the nematode protein do not support models on Sgt1 proteins binding only to the open state of Hsp90.[30,31,52] This is of relevance for the ATPase cycle of Hsp90 and the turnover of D1054.3-associated clients. D1054.3 can bind with low affinity to the open conformation of Hsp90 and is then able to change its binding mode to a high affinity interaction once Hsp90 closes its N-terminal domains

dx.doi.org/10.1021/bi5000542 | Biochemistry 2014, 53, 2505−2514

(Figure 6). This interaction could be influenced by further cofactors, such as the protein Rar1, which was shown to interact with Hsp90 and Sgt1 during the processing of NLRs.[52]

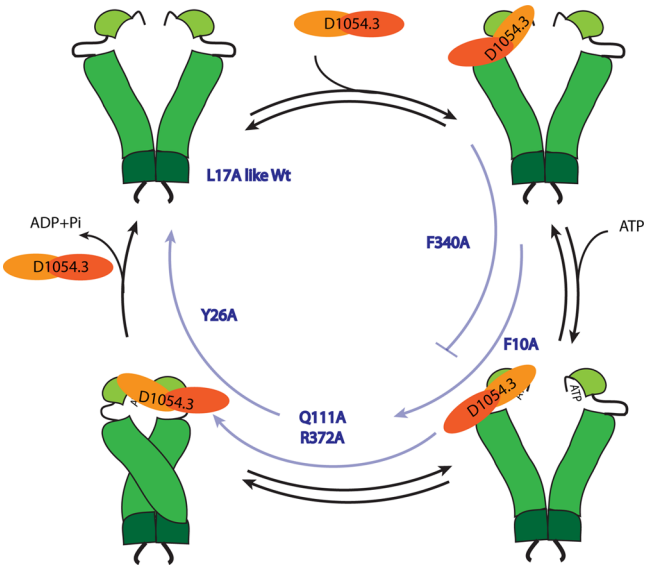

Figure 6. Illustrated model for the interaction between D1054.3 and Hsp90. In the model, the ATPase cycle of Hsp90 and the binding of D1054.3 to the closed and open state of Hsp90 are shown. The CS-domain of D1054.3 is depicted in orange and the SGS-domain is in red. Furthermore, the rate limiting step for each Hsp90 mutant is highlighted in blue.

The function of the SGS-domain in the context of client processing is not understood. This domain has been speculated to be an Hsc70 interaction site but could also be the binding site for clients such as the NLR proteins.[33] For the *C. elegans* system, we do not observe any interaction between Hsc70 and D1054.3 (data not shown). The TPR-domain has also been postulated to connect the chaperone machinery to clients and to the protein Skp1.[24,29] Our studies would challenge highly important contributions of the TPR-domain in Sgt1 amid its absence in many organisms. Furthermore, the TPR-domain was found to be dispensable for plant immunity and auxin signaling.[21,27,29,45,53]

Also information on the binding sites of D1054.3 could be obtained in our studies. Co-crystallization of the Hsp90 N-terminal domain with the CS-domain of Sgt1 revealed contact sites between the proteins; nevertheless, two potential binding sites remained possible.[31] As suggested by Zhang M. et al., residues in the N-terminal amino acid stretch modulate the binding to the open Hsp90 conformation.[31] Binding to the ATPγS-induced closed state is not as strongly affected by mutations at these sites. In the crystal structure reported before an interaction with the N-terminal amino acids is observable, suggesting that the crystallized interaction site reflects the binding to the open state, while the binding site in the closed state remains to be uncovered. Competition to Cep23 there is very strong. It will be interesting to see whether the interaction in the closed state exactly reflects the binding mode of p23. While sterical clashes with the TPR-domain were supposed to restrict this interaction in the mammalian system,[31] the nematode protein, lacking the TPR-domain, would allow the preferential formation of stable and more affine closed complexes.

■ ASSOCIATED CONTENT

Supporting Information

Three supplementary figures: Supplemental Figure 1. Purity and stability of the analyzed cochaperones. Supplemental Figure 2. Influence of p23 and D1054.3 on Hsp90. Supplemental Figure 3. Absence of interaction of D1054.3 with Hsp90MC and Hsp90M. This material is available free of charge via the Internet at http://pubs.acs.org.

■ AUTHOR INFORMATION

Corresponding Author

*Address: Department of Chemistry, Technische Universität München, Lichtenbergstrasse 4, 85748 Garching, Germany. Tel.: +49-089-289-13342. Fax: +49-089-289-13345. E-mail: klaus.richter@richterlab.de.

Funding

This work was supported by the Deutsche Forschungsgemeinschaft Grant RI1873/1-3.

Notes

The authors declare no competing financial interest.

■ ACKNOWLEDGMENTS

The authors thank Borries Demeler (University of San Antonio, Texas) for licenses to the UltraScan II and UltraScan III software packages. We would like to thank Katharina Papsdorf for critically reading the manuscript. J.E. acknowledges the support of the TUM Graduate School's Faculty Graduate Center of Chemistry at the Technische Universität München.

■ ABBREVIATIONS USED

aUC, analytical ultracentrifugation; IPTG, isopropyl-β-D-thiogalactopyranosid; SGS, SGT1-specific domain; CS, CHORD/SGT1 domain; TPR, tetratricopeptide domain; Cep23, *Caenorhabditis elegans* p23; CeAha1, *Caenorhabditis elegans* Aha1; Hsp90, heat shock protein 90; Cdc37, cell division cycle 37

■ REFERENCES

(1) Pearl, L. H., and Prodromou, C. (2006) Structure and mechanism of the Hsp90 molecular chaperone machinery. *Annu. Rev. Biochem. 75*, 271−294.

(2) Rohl, A., Rohrberg, J., and Buchner, J. (2013) The chaperone Hsp90: changing partners for demanding clients. *Trends Biochem. Sci. 38*, 253−262.

(3) Taipale, M., Krykbaeva, I., Koeva, M., Kayatekin, C., Westover, K. D., Karras, G. I., and Lindquist, S. (2012) Quantitative analysis of HSP90-client interactions reveals principles of substrate recognition. *Cell 150*, 987−1001.

(4) Eckl, J. M., and Richter, K. (2013) Functions of the Hsp90 chaperone system: lifting client proteins to new heights. *Int. J. Biochem. Mol. Biol. 4*, 157−165.

(5) Richter, K., Muschler, P., Hainzl, O., and Buchner, J. (2001) Coordinated ATP hydrolysis by the Hsp90 dimer. *J. Biol. Chem. 276*, 33689−33696.

(6) Ali, M. M., Roe, S. M., Vaughan, C. K., Meyer, P., Panaretou, B., Piper, P. W., Prodromou, C., and Pearl, L. H. (2006) Crystal structure of an Hsp90-nucleotide-p23/Sba1 closed chaperone complex. *Nature 440*, 1013−1017.

(7) Haslbeck, V., Eckl, J. M., Kaiser, C. J., Papsdorf, K., Hessling, M., and Richter, K. (2013) Chaperone-interacting TPR proteins in *Caenorhabditis elegans*. *J. Mol. Biol. 425*, 2922−2939.

(8) Wandinger, S. K., Richter, K., and Buchner, J. (2008) The Hsp90 chaperone machinery. *J. Biol. Chem. 283*, 18473−18477.

(9) Richter, K., Reinstein, J., and Buchner, J. (2007) A Grp on the Hsp90 mechanism. *Mol. Cell 28*, 177−179.
(10) Shiau, A. K., Harris, S. F., Southworth, D. R., and Agard, D. A. (2006) Structural Analysis of E. coli hsp90 reveals dramatic nucleotide-dependent conformational rearrangements. *Cell 127*, 329−340.
(11) Dollins, D. E., Warren, J. J., Immormino, R. M., and Gewirth, D. T. (2007) Structures of GRP94-nucleotide complexes reveal mechanistic differences between the hsp90 chaperones. *Mol. Cell 28*, 41−56.
(12) Ellis, R. J. (1998) Steric chaperones. *Trends Biochem. Sci. 23*, 43−45.
(13) Gano, J. J., and Simon, J. A. (2010) A proteomic investigation of ligand-dependent HSP90 complexes reveals CHORDC1 as a novel ADP-dependent HSP90-interacting protein. *Mol. Cell. Proteomics 9*, 255−270.
(14) Millson, S. H., Truman, A. W., King, V., Prodromou, C., Pearl, L. H., and Piper, P. W. (2005) A two-hybrid screen of the yeast proteome for Hsp90 interactors uncovers a novel Hsp90 chaperone requirement in the activity of a stress-activated mitogen-activated protein kinase, Slt2p (Mpk1p). *Eukaryotic Cell 4*, 849−860.
(15) Roe, S. M., Ali, M. M., Meyer, P., Vaughan, C. K., Panaretou, B., Piper, P. W., Prodromou, C., and Pearl, L. H. (2004) The Mechanism of Hsp90 regulation by the protein kinase-specific cochaperone p50(cdc37). *Cell 116*, 87−98.
(16) Vaughan, C. K., Gohlke, U., Sobott, F., Good, V. M., Ali, M. M., Prodromou, C., Robinson, C. V., Saibil, H. R., and Pearl, L. H. (2006) Structure of an Hsp90-Cdc37-Cdk4 complex. *Mol. Cell 23*, 697−707.
(17) Eckl, J. M., Rutz, D. A., Haslbeck, V., Zierer, B. K., Reinstein, J., and Richter, K. (2013) Cdc37 (cell division cycle 37) restricts Hsp90 (heat shock protein 90) motility by interaction with N-terminal and middle domain binding sites. *J. Biol. Chem. 288*, 16032−16042.
(18) Pearl, L. H. (2005) Hsp90 and Cdc37 – a chaperone cancer conspiracy. *Curr. Opin. Genet. Dev. 15*, 55−61.
(19) Pratt, W. B., and Toft, D. O. (1997) Steroid receptor interactions with heat shock protein and immunophilin chaperones. *Endocr. Rev. 18*, 306−360.
(20) Morishima, Y., Kanelakis, K. C., Murphy, P. J., Lowe, E. R., Jenkins, G. J., Osawa, Y., Sunahara, R. K., and Pratt, W. B. (2003) The hsp90 cochaperone p23 is the limiting component of the multiprotein hsp90/hsp70-based chaperone system in vivo where it acts to stabilize the client protein: hsp90 complex. *J. Biol. Chem. 278*, 48754−48763.
(21) Azevedo, C., Betsuyaku, S., Peart, J., Takahashi, A., Noel, L., Sadanandom, A., Casais, C., Parker, J., and Shirasu, K. (2006) Role of SGT1 in resistance protein accumulation in plant immunity. *EMBO J. 25*, 2007−2016.
(22) Bansal, P. K., Abdulle, R., and Kitagawa, K. (2004) Sgt1 associates with Hsp90: an initial step of assembly of the core kinetochore complex. *Mol. Cell. Biol. 24*, 8069−8079.
(23) Steensgaard, P., Garre, M., Muradore, I., Transidico, P., Nigg, E. A., Kitagawa, K., Earnshaw, W. C., Faretta, M., and Musacchio, A. (2004) Sgt1 is required for human kinetochore assembly. *EMBO Rep. 5*, 626−631.
(24) Kitagawa, K., Skowyra, D., Elledge, S. J., Harper, J. W., and Hieter, P. (1999) SGT1 encodes an essential component of the yeast kinetochore assembly pathway and a novel subunit of the SCF ubiquitin ligase complex. *Mol. Cell 4*, 21−33.
(25) Dubacq, C., Guerois, R., Courbeyrette, R., Kitagawa, K., and Mann, C. (2002) Sgt1p contributes to cyclic AMP pathway activity and physically interacts with the adenylyl cyclase Cyr1p/Cdc35p in budding yeast. *Eukaryotic Cell 1*, 568−582.
(26) Martins, T., Maia, A. F., Steffensen, S., and Sunkel, C. E. (2009) Sgt1, a co-chaperone of Hsp90 stabilizes Polo and is required for centrosome organization. *EMBO J. 28*, 234−247.
(27) Nyarko, A., Mosbahi, K., Rowe, A. J., Leech, A., Boter, M., Shirasu, K., and Kleanthous, C. (2007) TPR-Mediated self-association of plant SGT1. *Biochemistry 46*, 11331−11341.
(28) Bansal, P. K., Nourse, A., Abdulle, R., and Kitagawa, K. (2009) Sgt1 dimerization is required for yeast kinetochore assembly. *J. Biol. Chem. 284*, 3586−3592.
(29) Catlett, M. G., and Kaplan, K. B. (2006) Sgt1p is a unique co-chaperone that acts as a client adaptor to link Hsp90 to Skp1p. *J. Biol. Chem. 281*, 33739−33748.
(30) Takahashi, A., Casais, C., Ichimura, K., and Shirasu, K. (2003) HSP90 interacts with RAR1 and SGT1 and is essential for RPS2-mediated disease resistance in Arabidopsis. *Proc. Natl. Acad. Sci. U. S. A. 100*, 11777−11782.
(31) Zhang, M., Boter, M., Li, K., Kadota, Y., Panaretou, B., Prodromou, C., Shirasu, K., and Pearl, L. H. (2008) Structural and functional coupling of Hsp90- and Sgt1-centred multi-protein complexes. *EMBO J. 27*, 2789−2798.
(32) Shen, Q. H., Zhou, F., Bieri, S., Haizel, T., Shirasu, K., and Schulze-Lefert, P. (2003) Recognition specificity and RAR1/SGT1 dependence in barley Mla disease resistance genes to the powdery mildew fungus. *Plant Cell 15*, 732−744.
(33) Kadota, Y., and Shirasu, K. (2012) The HSP90 complex of plants. *Biochim. Biophys. Acta 1823*, 689−697.
(34) da Silva Correia, J., Miranda, Y., Leonard, N., and Ulevitch, R. (2007) SGT1 is essential for Nod1 activation. *Proc. Natl. Acad. Sci. U. S. A. 104*, 6764−6769.
(35) Noel, L. D., Cagna, G., Stuttmann, J., Wirthmuller, L., Betsuyaku, S., Witte, C. P., Bhat, R., Pochon, N., Colby, T., and Parker, J. E. (2007) Interaction between SGT1 and cytosolic/nuclear HSC70 chaperones regulates Arabidopsis immune responses. *Plant Cell 19*, 4061−4076.
(36) Spiechowicz, M., Zylicz, A., Bieganowski, P., Kuznicki, J., and Filipek, A. (2007) Hsp70 is a new target of Sgt1–an interaction modulated by S100A6. *Biochem. Biophys. Res. Commun. 357*, 1148−1153.
(37) Gaiser, A. M., Brandt, F., and Richter, K. (2009) The non-canonical Hop protein from Caenorhabditis elegans exerts essential functions and forms binary complexes with either Hsc70 or Hsp90. *J. Mol. Biol. 391*, 621−634.
(38) Gaiser, A. M., Kretzschmar, A., and Richter, K. (2010) Cdc37-Hsp90 complexes are responsive to nucleotide-induced conformational changes and binding of further cofactors. *J. Biol. Chem. 285*, 40921−40932.
(39) Richter, K., Soroka, J., Skalniak, L., Leskovar, A., Hessling, M., Reinstein, J., and Buchner, J. (2008) Conserved conformational changes in the ATPase cycle of human Hsp90. *J. Biol. Chem. 283*, 17757−17765.
(40) Panaretou, B., Prodromou, C., Roe, S. M., O'Brien, R., Ladbury, J. E., Piper, P. W., and Pearl, L. H. (1998) ATP binding and hydrolysis are essential to the function of the Hsp90 molecular chaperone in vivo. *EMBO J. 17*, 4829−4836.
(41) Sun, L., Edelmann, F. T., Kaiser, C. J., Papsdorf, K., Gaiser, A. M., and Richter, K. (2012) The lid domain of Caenorhabditis elegans Hsc70 influences ATP turnover, cofactor binding and protein folding activity. *PloS One 7*, e33980.
(42) Stafford, W. F., 3rd. (1992) Boundary analysis in sedimentation transport experiments: a procedure for obtaining sedimentation coefficient distributions using the time derivative of the concentration profile. *Anal. Biochem. 203*, 295−301.
(43) Brookes, E., Demeler, B., Rosano, C., and Rocco, M. (2010) The implementation of SOMO (SOlution MOdeller) in the UltraScan analytical ultracentrifugation data analysis suite: enhanced capabilities allow the reliable hydrodynamic modeling of virtually any kind of biomacromolecule. *Eur. Biophys. J. 39*, 423−435.
(44) Demeler, B., Brookes, E., Wang, R., Schirf, V., and Kim, C. A. (2010) Characterization of reversible associations by sedimentation velocity with UltraScan. *Macromol. Biosci. 10*, 775−782.
(45) Lingelbach, L. B., and Kaplan, K. B. (2004) The interaction between Sgt1p and Skp1p is regulated by HSP90 chaperones and is required for proper CBF3 assembly. *Mol. Cell. Biol. 24*, 8938−8950.
(46) Johnson, J. L., and Toft, D. O. (1995) Binding of p23 and hsp90 during assembly with the progesterone receptor. *Mol. Endocrinol. 9*, 670−678.

(47) Weaver, A. J., Sullivan, W. P., Felts, S. J., Owen, B. A., and Toft, D. O. (2000) Crystal structure and activity of human p23, a heat shock protein 90 co-chaperone. *J. Biol. Chem. 275*, 23045−23052.
(48) Prodromou, C., Panaretou, B., Chohan, S., Siligardi, G., O'Brien, R., Ladbury, J. E., Roe, S. M., Piper, P. W., and Pearl, L. H. (2000) The ATPase cycle of Hsp90 drives a molecular 'clamp' via transient dimerization of the N-terminal domains. *EMBO J. 19*, 4383−4392.
(49) McLaughlin, S. H., Sobott, F., Yao, Z. P., Zhang, W., Nielsen, P. R., Grossmann, J. G., Laue, E. D., Robinson, C. V., and Jackson, S. E. (2006) The co-chaperone p23 arrests the Hsp90 ATPase cycle to trap client proteins. *J. Mol. Biol. 356*, 746−758.
(50) Hessling, M., Richter, K., and Buchner, J. (2009) Dissection of the ATP-induced conformational cycle of the molecular chaperone Hsp90. *Nat. Struct. Mol. Biol. 16*, 287−293.
(51) Cunningham, C. N., Southworth, D. R., Krukenberg, K. A., and Agard, D. A. (2012) The conserved arginine 380 of Hsp90 is not a catalytic residue, but stabilizes the closed conformation required for ATP hydrolysis. *Protein Sci. 21*, 1162−1171.
(52) Zhang, M., Kadota, Y., Prodromou, C., Shirasu, K., and Pearl, L. H. (2010) Structural basis for assembly of Hsp90-Sgt1-CHORD protein complexes: implications for chaperoning of NLR innate immunity receptors. *Mol. Cell 39*, 269−281.
(53) Gray, W. M., Muskett, P. R., Chuang, H. W., and Parker, J. E. (2003) Arabidopsis SGT1b is required for SCF(TIR1)-mediated auxin response. *Plant Cell 15*, 1310−1319.